On Optimal Resource Allocation for Hybrid VLC/RF Networks With Common Backhaul

Vasilis K. Papanikolaou, *Student Member, IEEE*, Panagiotis D. Diamantoulakis, *Senior Member, IEEE*, Paschalis C. Sofotasios, *Senior Member, IEEE*, Sami Muhaidat, *Senior Member, IEEE*, and George K. Karagiannidis, *Fellow, IEEE*

***Abstract*—The synergy between visible light communication (VLC) and radio frequency (RF) networks has attracted a considerable amount of attention due to the envisioned improvements compared to conventional systems, mainly in terms of data rate and coverage. In this paper, we investigate for the first time the coexistence of VLC and RF networks, assuming that both networks are served by a common backhaul network, as well as both perfect and imperfect channel state information (CSI). In this context, we propose an optimal resource allocation scheme that maximizes the corresponding data rate, while also taking into account the fairness among the involved users. This is of paramount importance because in such heterogeneous networks, a standard rate maximization approach yields a severely degraded performance for the weaker users. In order to provide a tractable solution to the formulated problem, which is non-convex, we transform this into an equivalent convex one. Moreover, a simplified power allocation problem is solved, which provides comparable results with substantially lower complexity. Finally, extensive simulations illustrate the validity and effectiveness of the proposed analysis, and provide valuable insights on the impact of the imperfect CSI on the overall network performance.**

***Index Terms*—Visible light communications, hybrid VLC/RF, backhaul network, convex optimization, resource allocation, imperfect CSI, energy efficiency.**

I. Introduction

IN ORDER to address the demands of the next generation of wireless networks, considerable research and industrial activity has been devoted in recent years in understanding different regions of the electromagnetic spectrum with the aim to exploit them for resolving the expected spectrum scarcity and enabling massive connectivity. Such regions correspond primarily the mmWaves and the visible light spectrum. Based on this, with the inclusion of mmWaves in the IEEE 802.11ad standard for Wireless Fidelity (WiFi) and most importantly their use in the firth generation (5G) of wireless systems, it is natural to assume that a possible solution for the forthcoming "spectrum crunch" is to take advantage of those regions [2]–[5]. In the same context, it is also recalled that according to [6], around 80% of the mobile traffic originates from indoors. To this end, a promising technology for providing indoor data access is visible light communication (VLC), which takes advantage of the room illumination to offer particularly high data rates at a low cost. By exploiting a vast, unregulated, and free region of the electromagnetic spectrum, VLC can grant the necessary bandwidth to mitigate the excessive crowding and interference in the radio frequency (RF) communication systems. Also, the use of VLC is especially attractive for RF-sensitive applications, where RF radiation is considered harmful, such as for example in hospitals [3]. Moreover, the use of (light-emitting diodes) LED-based transmitters in VLC makes it an energy-efficient and relatively easy to implement technology. Furthermore, VLC offers superior physical layer security, since it is naturally confined in the room with the light source [3].

However, the main drawback of the VLC networking solution is its limited coverage capability, since the optical link can be easily interrupted by random movement and/or rotation of the receiver. On the contrary, RF-based solutions can, in fact, achieve ubiquitous coverage. Also, effective VLC-based uplink transmission is still under investigation; as a result, an RF-based uplink is typically considered in most cases in the state-of-the-art. Consequently, heterogeneous networking could capitalize on both technologies' advantages so that hybrid systems with coordinated use of VLC and RF can fully exploit the system capacity, while ensuring high coverage. It is evident that the successful deployment of this synergy has the potential to effectively support the continuously increasing quality of service (QoS) requirements.

A. State-of-the-Art

The recent research activity on the optimization of hybrid VLC/RF networks has yielded several interesting contributions, e.g., [7]–[22] - and the references therein. More specifically, the authors in [7] investigated the area spectral

Manuscript received December 28, 2018; revised July 27, 2019 and October 28, 2019; accepted December 4, 2019. Date of publication January 3, 2020; date of current version March 6, 2020. This work was supported in part by Khalifa University under Grant KU/FSU-8474000122 and Grant KU/RC1-C2PS-T2/8474000137. This paper was presented in part at IEEE Wireless Communications and Networking Conference 2018 (IEEE WCNC'18) [1]. The associate editor coordinating the review of this article and approving it for publication was H. Haas. *(Corresponding author: Panagiotis D. Diamantoulakis.)*

Vasilis K. Papanikolaou, Panagiotis D. Diamantoulakis, and George K. Karagiannidis are with the Department of Electrical and Computer Engineering, Aristotle University of Thessaloniki, 54636 Thessaloniki, Greece (e-mail: vpapanikk@auth.gr; padiaman@ieee.org; geokarag@auth.gr).

Paschalis C. Sofotasios is with the Center for Cyber Physical Systems, Department of Electrical Engineering and Computer Science, Khalifa University, Abu Dhabi, UAE, and also with the Department of Electrical Engineering, Tampere University, 33101 Tampere, Finland (e-mail: p.sofotasios@ieee.org).

Sami Muhaidat is with the Center for Cyber Physical Systems, Department of Electrical Engineering and Computer Science, Khalifa University, Abu Dhabi, UAE (e-mail: sami.muhaidat@ku.ac.ae).

Digital Object Identifier 10.1109/TCCN.2019.2963879

efficiency, taking into account user association in a three-tier hybrid VLC/RF network considering macro-, femto- and optical attocells. In [8], the aggregated serving of users from both the VLC and the RF systems in a hybrid network has been considered. In the same context, an RF network is presented in [16] as complementary to VLC, which subsequently forms a hybrid VLC/RF configuration that improves the outage probability.

However, despite the paramount importance of channel estimation errors due to their detrimental effects, analyses with the assumption of imperfect channel state information (CSI) in VLC networks are limited in the existing literature [23]–[25]. Specifically, the authors in [23] analyzed a VLC broadcasting network under imperfect CSI. Furthermore, in [24] and [25], a multiuser VLC mulitple-input multiple-output (MIMO) system with imperfect CSI has been investigated. Nevertheless, despite the prominence of hybrid VLC/RF networks, to the best of the authors' knowledge, the effect of imperfect CSI on the overall network performance has not been investigated before.

It is also recalled that in coordinated Heterogeneous Networks (HetNets), such as the hybrid VLC/RF network, numerous challenges need to be addressed in order to ensure fairness among users. Furthermore, in hybrid VLC/RF networks there is also the need for new coordination and resource allocation schemes in order to optimize the load balancing of the network. Specifically, effective handover schemes, between the two networks, due to VLC's limited coverage, need to be designed to ensure full time connectivity. These cases have been studied extensively in recent years [9]–[14]. In more detail, Markov decision process was used to study the vertical handovers between the VLC and RF networks in [9]. In [10], an optimization framework was developed in order to maximize throughput and user fairness in a dynamic load balancing scheme, while in [11] a cooperative load balancing scheme was investigated in order to optimize user fairness. In [12], fuzzy logic was employed to associate users with either the RF AP or the VLC AP. Then, the access point selection takes place in the same manner as it would in a homogeneous network, VLC or RF, while evolutionary game theory was applied to provide the load balancing implementation. In [14], two algorithms were proposed for the optimization of access point selection, which were also compared with each other in terms of fairness, data rate and complexity, considering the user mobility. In [18], the RF part of the HetNet was considered in the context of a WiFi network and the hybrid network was designed and experimentally tested. More recently, the authors of [19] used learning methods, such as the multi-armed bandit model for decision making, to optimize the access point selection. In [20], a hybrid VLC/RF network was studied as a software defined network (SDN) and was optimized with respect to energy efficiency and inter-cell interference. Likewise, Hammouda *et al.* presented a cross-layer analysis of the physical and data-link layers for the hybrid VLC/RF networks in [21]. Also, the authors of [22] examined the co-existence of the two networks in terms of coverage probability. Moreover, the work of Abdelhady *et al.*, which focuses on resource allocation for a pure VLC network with time division multiple access (TDMA) provided valuable insights for the design of hybrid VLC/RF networks [26].

Finally, VLC/RF networks have been investigated with respect to wireless power transfer capabilities [27]. In [15], a hybrid network that employs energy harvesting is studied in terms of secrecy outage probability. The authors of [17] studied a hybrid VLC/RF network with a solar panel as a relay that harvests optical energy from the VLC system and performs decode and forward operations via an RF link to the users. Also, the performance of a hybrid RF/VLC ultra-small cell network with simultaneous lightwave information and power transfer (SLIPT) in [28] and energy transfer over the RF band was optimized in [29], assuming multiple users and optical angle-diversity transmitters.

However, the effect of the limitation concerning the common backhaul network has not been considered in any of the aforementioned contributions. In general, except for Ethernet, a big range of backhaul technologies and designs can be used, each of which comes with different installation costs and achievable performance. In [30], the use of power line communication (PLC) has been considered as a backhaul network for the VLC part, since it can be cost-effective. In fact, the proposed analysis considers PLC because of the convenience provided by its ubiquitous indoors presence. However, while PLC offers several advantages, primarily due to its easy implementation (Plug & Play), it suffers from frequency selective channel gain, limited bandwidth, and non-Gaussian noise. Therefore, another proposed implementation for the backhaul network in the state-of-the-art is the conventional optical fiber [31]. Moreover, optical wireless communication could also constitute a viable solution for the backhaul [32], [33].

The joint design of the backhaul and the hybrid VLC/RF communication system with orthogonal frequency division multiplexing has been investigated by [34], [35], for a single-user and multi-user system, respectively, assuming that the VLC and RF subsystems use different backhaul links with disjoint rates and perfect channel state information (CSI). More specifically, in [34], the authors investigated how a PLC backhaul for the VLC affects the hybrid VLC/RF network setup, when the aim is to maximize the total rate by optimizing the transmit power at each of them. On the other hand, in [35] the weighted sum rate has been optimized, assuming though that each of the subsystems (i.e., VLC and RF) can offer a fixed sum rate, which does not depend on the conditions of the wireless channels. Thus, the main focus of [35] was solely on the optimization of the information transmission over the backhaul link.

B. Motivation and Contribution

In a realistic scenario, the hybrid VLC/RF network will be served by a single backhaul infrastructure, since a common subscription line would be available from the network provider. Also, in contrast to [35], where it was assumed that all users can be simultaneously served by both subsystems, in this paper we assumed that each user is served solely by one subsystem. This assumption is more practical, since, for

the same user, one subsystem will usually dominate the other due to fundamentally different wireless propagation characteristics, while carrier aggregation in such disjoint bands is still an open issue. Thus, fairness between the users of the two subsytems becomes of paramount importance, due to the impact of the heterogeneous wireless channels of the two subsystems on performance. To the best of the authors' knowledge, this practical scenario has not been sufficiently investigated in the state-of-the-art. Moreover, it is worth noting that the commonly used assumption of perfect CSI is rarely satisfied in practice, due to feedback delays and position changes. Motivated by this, in this paper, the effect of channel estimation errors in the hybrid VLC/RF network is considered. To this end, the joint resource allocation problem of a multi-user coordinated VLC/RF network is investigated, under the practical assumptions of a common backhaul network for the two subsystems, as well as imperfect channel estimation, in both VLC and RF networks. Also, resource allocation in such a HetNet needs to guarantee user fairness, since VLC users can accumulate the available capacity offered from the backhaul network, at the expense of the quality of service (QoS) of the RF users. However, channel estimation errors affect significantly the performance of the involved users; hence, depending on their severity, the distribution of resources in the hybrid network needs to be controlled accordingly in order to ensure the required fairness. We note that this paper is an extension of our conference paper [1]. Although a similar problem has been investigated in [1], the provided solution was derived assuming perfect CSI and only power allocation. Thus, the contributions of this paper are summarized below:

- An optimization framework is developed that guarantees fair allocation of the available resources of the RF and VLC subsystems, i.e., power, bandwidth, and time, when the total rate is also limited by the backhaul capacity, for both the cases of perfect and imperfect CSI availability at the transmitter. More specifically, a joint resource allocation algorithm is designed that efficiently achieves the maximization of proportional fairness.
- The effect of imperfect CSI on the optimal resource allocation at each subsystem is quantified and evaluated.
- A simplified resource allocation framework is designed based on equal distribution of time and bandwidth resources to users, which effectively lowers the complexity of the original optimization problems.
- Simulation results are presented to validate the proposed analysis, while some interesting remarks are offered concerning the operation of the hybrid VLC/RF network. It is shown that in the case of a low backhaul capacity, both the VLC and the RF systems seem to operate at similar data rates. However, in cases in which the backhaul network offers higher capacity, the VLC can enable even higher data rates, while the RF system reaches a ceiling. Moreover, the effectiveness of the simplified problem is proven, showing comparable results with substantially lower complexity.

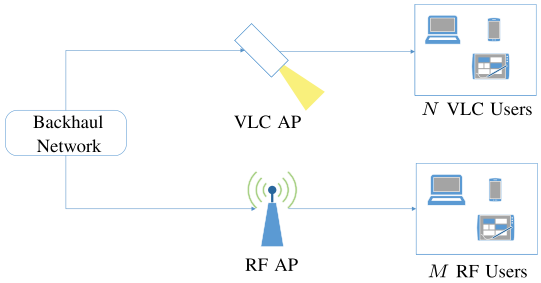

Fig. 1. VLC and RF sharing the same backhaul network.

C. Structure

The remainder of the paper is organized as follows: In Section II, the system model is presented and described. In Section III, the problem is formulated and transformed to a convex one. The algorithm to solve via convex optimization methods is analyzed in III-C along with the special case of perfect CSI. In Section IV, a simplified resource allocation scheme is examined, based on the peculiarities of the problem described in III. Finally, simulation results that show the validity of the proposed analysis are presented in Section V, while a conclusion is drawn in Section VI.

II. System Model

We consider the downlink transmission of a coordinated VLC/RF network, consisting of one VLC access point (AP), one RF AP, and multiple users, as illustrated in Fig. 1. In this setup, we assume two users groups, with $\mathcal{N} = \{1, \ldots, n, \ldots, N\}$ and $\mathcal{M} = \{1, \ldots, m, \ldots, M\}$ served by the VLC and RF AP, respectively. Furthermore, we assume that the two networks share the same backhaul, the capacity of which is fixed and equal to C_0, as also depicted in Fig. 1. In addition, it is assumed that all mobile nodes are equipped with single antennas/photo-detectors and each user utilizes solely an orthogonal communication channel, with B, t and w, τ denoting its bandwidth and timeslot duration for the VLC and RF systems, respectively.

It is also assumed that TDMA and frequency division multiple access (FDMA) are used for the VLC and RF system, respectively [36], [37]. However, the following analysis is not restricted as it is directly applicable to different multiple access schemes. Note that the use of TDMA for VLC has been considered in the literature [16], [26], because of its low complexity. Thus, B corresponds to the bandwidth of the VLC system, t_n represents the timeslot of user n of the VLC system, w_m denotes the bandwidth of user m of the RF system, and $\tau = T$, where T is the corresponding transmission frame period. Finally, the present analysis focuses on the downlink scenario, but it is readily applicable to the uplink case as well.

A. The VLC Sub-Network

1) Channel Model: Without loss of generality, a line-of-sight (LoS) link is assumed to be always available for VLC users; hence, according to [38], the NLoS component offers only a small increase in the received power [16], [17], [33]. It

should be noted though that the presented mathematical analysis is also valid for the case of both LoS and NLoS channel gains. Thus, the channel power gain is given by [23], [38]

$$h_n = \frac{L_r}{d_n^2} r_0(\varphi)\, T_s(\psi) g(\psi) \cos(\psi), \tag{1}$$

where L_r is the physical area of the photo-detector, d_n is the transmission distance from the LED to the illuminated surface of the *n*-th user's photo-detector, $T_s(\psi)$ is the gain of the optical filter and $g(\psi)$ represents the gain of the optical concentrator, given by [38] and [39], namely

$$g(\psi) = \begin{cases} \frac{n_c^2}{\sin^2(\Psi_{\rm fov})}, & 0 \le \psi \le \Psi_{\rm fov}, \\ 0, & \psi > \Psi_{\rm fov}, \end{cases} \tag{2}$$

with n_c and $\Psi_{\rm fov}$ denoting the refractive index and FOV, respectively. Also in (1), $r_0(\varphi)$ is the Lambertian radiant intensity of the LED, given by

$$r_0(\varphi) = \frac{\xi + 1}{2\pi} \cos^{\xi} \varphi, \tag{3}$$

where φ is the irradiance angle, ψ is the incidence angle, and

$$\xi = -\frac{1}{\log_2 \cos\Big(\Phi_{1/2}\Big)}, \tag{4}$$

with $\Phi_{1/2}$ denoting the semi-angle at half luminance.

Assuming a channel estimation $\hat{h}_n$ between the *n*-th user and the AP, it follows that [25]

$$\hat{h}_n = h_n + \delta_n, \tag{5}$$

where δ_n denotes the channel estimation error modeled as a zero-mean Gaussian random variable with variance σ_δ^2, i.e., $\delta \sim \mathcal{N}(0, \sigma_\delta^2)$. It is noted here that (5) has been adopted for indoor VLC systems and is represented as [25]

$$h_n = \rho_n \hat{h}_n + \epsilon_n, \tag{6}$$

where $\rho_n = \mathbb{E}[\hat{h}_n h_n] = \sigma_{h_n}^2 / \sigma_{\hat{h}_n}^2$, while $\sigma_\epsilon^2 = (1 - \rho_n)\sigma_{h_n}^2$ [40]. It is noted here that $\sigma_{h_n}^2$ and $\sigma_{\hat{h}_n}^2$ are the variances of the actual channel and its estimate, respectively. To give further insight on this, according to the principal of orthogonality, the channel estimator (i.e., least mean squares estimator) yields an estimation error that is orthogonal to the channel realization *h*, as it can be seen in Fig. 2. Also, we adopt the reasonable assumption that the channel estimation error follows the same distribution for all VLC users. The baseband equivalent of the received signal, *y*, can then be expressed as

$$y = hx + w = \rho \hat{h} x + \epsilon x + w, \tag{7}$$

where ϵ is a random variable, *x* is the transmitted signal, and *w* denotes the additive noise component.

2) Achievable Rate: Assuming the use of intensity modulation direct detection (IM/DD) scheme, the achievable rate of the *n*-th user can be expressed by using a lower bound of the capacity in [41], namely

$$R_n^{[\rm VLC]} = t_n B \log_2\Big(1 + \frac{e}{2\pi} \gamma_n^{[\rm VLC]}\Big), \tag{8}$$

where *B* is the bandwidth of the VLC system, t_n is the transmission timeslot of user *n*, and $\gamma_n^{[\rm VLC]}$ is the received SNR,

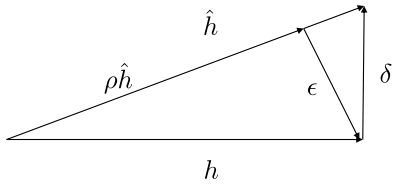

Fig. 2. Orthogonality principle of channel estimation error.

which can be expressed as [11]

$$\gamma_n^{[\rm VLC]} = \frac{\Big(\rho_n \hat{h}_n \eta P_n\Big)^2}{\sigma^2 + \sigma_\epsilon^2 \eta^2 P_n^2}. \tag{9}$$

In (9), P_n is the transmitted optical power to the *n*-th user, σ^2 is the noise power and, η denotes the photodetector's responsivity. It is recalled that the denominator of the SNR is the sum of noise variances if we adopt the common and reasonable assumption that Gaussian codebooks are used.

Note that, the achievable rate of the VLC system is also limited by the average optical power (lighting constraint), i.e.,

$$\sum_{n=1}^{N} t_n P_n \le t P_{\rm av}, \tag{10}$$

and also by the maximum duration of timeslot constraint *t*, i.e.,

$$\sum_{n=1}^{N} t_n \le t. \tag{11}$$

B. The RF Sub-Network

The path loss factor of the link between the RF AP to user *m* is denoted by L_m, and it is given by [16] as

$$L(d_m) = L(d_0) + 10\kappa \log_{10}(d_m / d_0), \tag{12}$$

where $L(d_0) = 68$ dB is the reference path loss at a reference distance, d_m is the distance between the RF AP and the *m*-th RF user, $d_0 = 1$ m, and $\kappa = 1.6$ is the corresponding path loss exponent. Moreover, the term related to the small scale fading for the *m*-th user is given by the complex random variable $h_m \sim \mathcal{CN}(0, 1)$ and frequency flat fading is assumed. Similar to the VLC part of the system, we also assume imperfect CSI at the RF receiver. Accordingly, we assume the variance of the channel estimation error to be

$$\sigma_\zeta^2 = \Big(1 - \mathbb{E}\Big[\hat{h}_m h_m\Big]\Big)\sigma_{h_m}^2 = (1 - \rho_m)\sigma_{h_m}^2. \tag{13}$$

Based on this, the achievable rate can be written as

$$R_m^{[\rm RF]} = T w_m \log_2\left(1 + \frac{L_m \Big|\rho_m \hat{h}_m\Big|^2 p_m}{N_0 w + \sigma_\zeta^2 L_m p_m}\right), \tag{14}$$

where N_0 is the power spectral density of the white noise for the RF system. Also, concerning power and bandwidth limitations, the following constraints, need to be satisfied

$$\sum_{m=1}^{M} p_m \le p_{\max}, \tag{15}$$

and

$$\sum_{m=1}^{M} w_m \leq w, \tag{16}$$

respectively.

III. Resource Allocation

In this section a joint resource allocation problem is formulated for a hybrid VLC/RF network, when both the VLC network and the RF network share the same backhaul infrastructure.

A. Proportional Fairness

In resource allocation problems within HetNets, different network attributes affect the QoS of the involved users. In this particular HetNet, the VLC subsystem can provide significantly higher data rates to its users; as a consequence, the conventional sum rate maximization of the system will potentially lead to a solution where the VLC users accumulate the largest part of the system's capacity, offered by the common backhaul, and let the RF users with low QoS. In general, various fairness metrics have been introduced in similar problems where an effective compromise between overall sum rate and user fairness needs to be achieved. In this work, the proportional fairness metric [11], [12] is used, being defined as the logarithm of the utility function of the users. In this scenario, the utility of the users is measured by their achieved data rate, thus reducing the proportional fairness of a system to the sum of the logarithm of the data rates (sum–log–rate). Consequently, the proportional fairness of the VLC and RF network can be expressed as

$$\mathrm{PF}_{\mathrm{VLC}} = \sum_{n=1}^{N} \log\left(\beta_n\right) \tag{17}$$

and

$$\mathrm{PF}_{\mathrm{RF}} = \sum_{m=1}^{M} \log\left(\delta_m\right), \tag{18}$$

respective, where β_i and δ_i denote the utility function of the *i*-th user of the corresponding subsystem.

In this context, we introduce a weighted sum of (17) and (18) as the weighted proportional fairness of the hybrid VLC/RF network, which yields

$$\mathrm{PF} = \alpha \sum_{n=1}^{N} \log\left(\beta_n\right) + (1-\alpha) \sum_{m=1}^{M} \log\left(\delta_m\right), \tag{19}$$

where $0 \leq \alpha \leq 1$ is the aforementioned weight. Similarly to the sum rate maximization, the proportional fairness is also an increasing function of each user's data rate. In addition, the logarithm is used for its property to tend to negative infinity when its argument tends to zero. Thus, solutions offering very low data rates to some users will yield significantly lower proportional fairness.

B. Problem Formulation

In this setting, a resource allocation (RA) problem is investigated for the hybrid VLC/RF network. The following analysis aims at maximizing the proportional fairness of the users with regards to the power allocated at each user. Also, for the VLC users that employ TDMA, the time-frame of each user is optimized; similarly, the bandwidth allocated to each RF user, since FDMA is employed in the RF network, is also optimized. Finally, the parameter $0 \leq \alpha \leq 1$ is used as a weight to potentially give priority to one subsystem of the hybrid network over the other. Based on these characteristics, the corresponding optimization problem can be formulated as

$$\begin{aligned}
\max_{\mathbf{P},\mathbf{p},\mathbf{t},\mathbf{w}} \quad & \alpha \sum_{n=1}^{N} \log\left(R_n^{[\mathrm{VLC}]}\right) + (1-\alpha) \sum_{m=1}^{M} \log\left(R_m^{[\mathrm{RF}]}\right) \\
\mathbf{s.t.} \quad & \mathrm{C}_1 : \sum_{n=1}^{N} R_n^{[\mathrm{VLC}]} + \sum_{m=1}^{M} R_m^{[\mathrm{RF}]} \leq C_0, \\
& \mathrm{C}_2 : \sum_{n=1}^{N} t_n P_n \leq t P_{\mathrm{av}}, \\
& \mathrm{C}_3 : \sum_{m=1}^{M} p_m \leq p_{\max}, \\
& \mathrm{C}_4 : \sum_{n=1}^{N} t_n \leq t, \\
& \mathrm{C}_5 : \sum_{m=1}^{M} w_m \leq w.
\end{aligned} \tag{20}$$

In (20), the vectors **P**, **p**, **t**, **w** denote the sets of P_n, p_m, t_n, w_m, respectively. The first constraint ensures that the total data rate of both VLC and RF is less than the capacity of the backhaul network. Moreover, the maximum allowable power consumption levels of both systems are constrained by the physical limitations of the APs, leading to the constraints C_2 and C_3. Furthermore, constraints C_4 and C_5 are related to the utilized multiple access technique in each system. Since TDMA is employed in VLC, each user is served in a different timeslot within a frame, the total duration of which is denoted by *t*. Similarly, with the use of FDMA for the RF system, the fractions of bandwidth that are allocated to different users cannot exceed *w*, which is defined as the total bandwidth that has been preassigned to the RF subsystem.

It is noted that the optimization problem in (20) is non-convex. The main reasons of non-convexity are the imperfect CSI at the transmitter, the expression for the capacity in VLC with IM/DD, and the assumption of limited backhaul. More specifically, to give further insight on this, it needs to be mentioned that when the Shannon's formula is used and perfect CSI is available at the transmitter, the multiplication of the allocated bandwidth with the logarithmic function of power is a convex function, since the bandwidth variable of frequency also appears in the denominator, due to its multiplication with the noise power. Although the same does not hold when time is the resource of interest instead of frequency, e.g., when TDMA is used, this is often resolved by replacing the variable of power with energy, i.e., the multiplication of time with power [42]. However, this transformation is not adequate for this specific problem. This is because the achievable rate for the VLC is non-concave due to the squared term of optical power. Also, both expressions of the rate are non-concave due to the inclusion of the power in the denominator.

TABLE I
NOTATION FOR THE TRANSFORMED PROBLEM

Original problem	Equivalent transformed problem
Expression for rate for VLC user n, $R_n^{[\mathrm{VLC}]}$	Auxiliary variable for rate $r_n^{\mathrm{VLC}} \leq R_n^{[\mathrm{VLC}]}$
Rate of VLC user n, r_n^{VLC}	$\exp(\tilde{r}_n^{\mathrm{VLC}}) = r_n^{\mathrm{VLC}}$
Expression for rate for RF user m, $R_m^{[\mathrm{RF}]}$	Auxiliary variable for rate $r_m^{\mathrm{RF}} \leq R_m^{[\mathrm{RF}]}$
Rate of RF user m, r_m^{RF}	$\exp(\tilde{r}_m^{\mathrm{RF}}) = r_m^{\mathrm{RF}}$
Power of VLC user n, P_n	$\exp(\tilde{P}_n) = P_n$
Power of RF user m, p_m	$\exp(\tilde{p}_m) = p_m$
Timeslot duration of VLC user n, t_n	$\exp(\tilde{t}_n) = t_n$
Bandwidth of RF user m, w_m	$\exp(\tilde{w}_m) = w_m$

Moreover, even if both expressions of the rate were concave, the problem would still be non-convex due to C_1 of (18), which, in this case, would limit the maximum value of the sum of concave functions, which is also a concave function, instead of a convex one as it would be required to preserve convexity. Moreover, C_2 is non-convex due to the multiplication of t_n with p_n. Therefore the complexity to solve it is high, mainly due to the relation of the rates with the power allocation variables. Therefore, it is important to prove, that the problem in (20) can be transformed to a convex one; so, the process to find a global maximum can be solved in polynomial time, in order to derive a tractable resource allocation algorithm to ensure proportional fairness.

Proposition 1: The optimization problem in (20) can be formulated as a convex one.

Proof: The proof is provided in the Appendix. ∎

Following Proposition 1, the equivalent convex problem of (20) can be expressed as follows:

$$\begin{aligned}
\max_{\substack{\tilde{\mathbf{P}},\tilde{\mathbf{p}},\\ \tilde{\mathbf{t}},\tilde{\mathbf{w}},\tilde{\mathbf{r}}^{\mathrm{VLC}},\tilde{\mathbf{r}}^{\mathrm{RF}}}} \quad & \alpha \sum_{n=1}^{N} \tilde{r}_n^{\mathrm{VLC}} + (1-\alpha) \sum_{m=1}^{M} \tilde{r}_m^{\mathrm{RF}} \\
\text{s.t.} \quad & \mathrm{C}_1 : \sum_{n=1}^{N} \exp\left(\tilde{r}_n^{\mathrm{VLC}}\right) + \sum_{m=1}^{M} \exp\left(\tilde{r}_m^{\mathrm{RF}}\right) \leq C_0, \\
& \mathrm{C}_2 : \sum_{n=1}^{N} e^{\tilde{P}_n + \tilde{t}_n} \leq t P_{\mathrm{av}}, \\
& \mathrm{C}_3 : \sum_{m=1}^{M} e^{\tilde{p}_m} \leq p_{\max}, \\
& \mathrm{C}_4 : \sum_{n=1}^{N} e^{\tilde{t}_n} \leq t, \\
& \mathrm{C}_5 : \sum_{m=1}^{M} e^{\tilde{w}_m} \leq w, \\
& \mathrm{C}_6 : \log\Big(2^{\exp(\tilde{r}_n^{\mathrm{VLC}} - \tilde{t}_n)/B} - 1\Big) \\
& \qquad + \log\Big(\sigma_\epsilon^2 \eta^2 + \sigma^2 \exp\Big(-2\tilde{P}_n\Big)\Big) \\
& \qquad \leq \log\left(\frac{e h_n^2 \eta^2}{2\pi}\right), \quad \forall n \in \mathcal{N}, \\
& \mathrm{C}_7 : \log\Big(2^{\exp(\tilde{r}_m^{\mathrm{RF}} - \tilde{w}_m)/T} - 1\Big) \\
& \qquad + \log\Big(\sigma_\zeta^2 L_m + N_0 \exp(\tilde{w}_m - \tilde{p}_m)\Big) \\
& \qquad \leq \log\Big(|h_m|^2 L_m\Big), \quad \forall m \in \mathcal{M}. \qquad (21)
\end{aligned}$$

For the reader's convenience, the changes on variables are shown in Table I.

In (21), C_1 represents the limited capacity offered from the shared backhaul network, while C_2 and C_3 include the hardware limitations of the APs for power consumption. C_4 and C_5 are related to the multiple access techniques and the limitations for the timeslot and bandwidth of each system. Finally, C_6 and C_7 are imposed by (49), according to which the achieved rate for each user cannot exceed the capacity of the corresponding links over the VLC and RF subsystems.

1) The Special Case of Perfect CSI: As a special case, the resource allocation problem is studied when perfect CSI is assumed. This means that the channel estimation and the channel have a correlation of 1, so the variance of channel estimation error is 0. This observation transforms the optimization problem in (21) to the following one:

$$\begin{aligned}
\max_{\substack{\tilde{\mathbf{P}},\tilde{\mathbf{p}},\\ \tilde{\mathbf{t}},\tilde{\mathbf{w}},\tilde{\mathbf{r}}^{\mathrm{VLC}},\tilde{\mathbf{r}}^{\mathrm{RF}}}} \quad & \alpha \sum_{n=1}^{N} \tilde{r}_n^{\mathrm{VLC}} + (1-\alpha) \sum_{m=1}^{M} \tilde{r}_m^{\mathrm{RF}} \\
\text{s.t.} \quad & (21).\mathrm{C}_1,\ (21).\mathrm{C}_2,\ (21).\mathrm{C}_3,\ (21).\mathrm{C}_4,\ (21).\mathrm{C}_5 \\
& \mathrm{C}_6 : -\tilde{P}_n + \frac{1}{2}\log\left(\frac{2^{\exp(\tilde{r}_n^{\mathrm{VLC}} - \tilde{t}_n)/B} - 1}{G_n^2}\right) \\
& \qquad \leq 0, \quad \forall n \in \mathcal{N}, \\
& \mathrm{C}_7 : -\tilde{p}_m + \log\left(\frac{2^{\exp(\tilde{r}_m^{\mathrm{RF}} - \tilde{w}_m)/T} - 1}{A_m^2}\right) \\
& \qquad + \tilde{w}_m \leq 0, \quad \forall m \in \mathcal{M}, \qquad (22)
\end{aligned}$$

where G_n is given by $G_n^2 = \frac{e h_n^2 \eta^2}{2\pi\sigma^2}$ and A_m is given by $A_m^2 = \frac{L_m |h_m|^2}{N_0}$. It is evident that the optimization problem in (22) is also convex.

C. Proposed Solution

Due to their convexity, the optimization problems in (21) and (22) can be solved by a decomposition method. Although their objective function can be decoupled to smaller subproblems, that's not the case for the constraints. As a result, primal decomposition methods are not appropriate for this method. To this end, the following considerations emerge:

- A dual decomposition method is required to solve this problem because the constraints cannot be decoupled, since the backhaul capacity is shared between the networks. Any solution that would arbitrarily share the available C_0 would be suboptimal.
- As it is analytically shown in the proof of Proposition 1, the maximization problem in (21) is convex, since the

objective function is jointly concave with respect to all the optimization variables, the left terms of the constraints are convex, and it satisfies the Slater's constraint qualification. Thus, the duality gap between the dual and the primal solution is zero [43]. Thus, the solution of the dual problem leads to the optimal solution of the original problem.

Based on the above, we solve (21) using the Lagrange dual decomposition method, and we obtain the Lagrangian of the problem, which is given by (23), as shown at the bottom of this page, with λ_i being the Lagrange multipliers (LMs).

In each iteration, the subproblems of resource allocation is solved in Layer 1 by using the Karush-Kuhn-Tucker (KKT) conditions for a fixed set of LMs, which are updated in Layer 2. For this purpose, the subgradient method is used, which is a well-accepted method for facilitating resource allocation in wireless communication systems and provides a theoretical complexity of $O(1/\epsilon^2)$ iterations to find ϵ-suboptimal point [44]. This two layer approach enables the different resource allocation subproblems for each subsystem and user and to be solved in parallel, requiring only knowledge of the updated values of the LMs. Moreover, it reduces the required computational and memory resources. In what follows, the two layers are explained in detail.

1) Layer 1: According to Karush-Kuhn-Tucker (KKT) conditions [43], the optimal values can be obtained by taking the first derivatives and setting them equal to zero. Consequently the following expressions hold $\forall n \in \mathcal{N}$ and $\forall m \in \mathcal{M}$:

$$\begin{aligned}\frac{\partial L}{\partial \tilde{P}_n} &= 0 \Leftrightarrow \lambda_2 \exp(\tilde{t}_n)\left(\sigma_\epsilon^2\eta^2\exp\left(3\tilde{P}_n\right)+\sigma^2\exp\left(\tilde{P}_n\right)\right)\\ &= 2\sigma^2\lambda_{5+n}, \end{aligned} \tag{24}$$

$$\begin{aligned}\frac{\partial L}{\partial \tilde{p}_m} &= 0 \Leftrightarrow \lambda_3\left(\exp\left(2\tilde{P}_n\right)\sigma_\zeta^2 L_m + N_0\exp(\tilde{w}_m+\tilde{p}_m)\right)\\ &= \lambda_{5+N+m}N_0\exp(\tilde{w}_m), \end{aligned} \tag{25}$$

$$\begin{aligned}\frac{\partial L}{\partial \tilde{t}_n} &= 0 \Leftrightarrow \frac{\lambda_{5+n}2^{\left(\tilde{r}_n^{\mathrm{VLC}}-\tilde{t}_n\right)/B}}{2^{\left(\tilde{r}_n^{\mathrm{VLC}}-\tilde{t}_n\right)/B}-1}\\ &= \frac{2B^2\exp\left(-\tilde{r}_n^{\mathrm{VLC}}\right)\left(\lambda_4+\lambda_2 e^{\tilde{P}_n}\right)}{\exp\left(-2\tilde{t}_n\right)\log(2)}, \end{aligned} \tag{26}$$

$$\begin{aligned}\frac{\partial L}{\partial \tilde{r}_n^{\mathrm{VLC}}} &= 0 \Leftrightarrow \lambda_1\exp\left(\tilde{r}_n^{\mathrm{VLC}}\right)+\lambda_{5+n}\\ &\quad\times\frac{\exp\left(\tilde{r}_n^{\mathrm{VLC}}-\tilde{t}_n\right)\log(2)2^{\exp\left(\tilde{r}_n^{\mathrm{VLC}}-\tilde{t}_n\right)/B}}{2B\left(2^{\exp\left(\tilde{r}_n^{\mathrm{VLC}}-\tilde{t}_n\right)/B}-1\right)}=\alpha, \end{aligned} \tag{27}$$

$$\begin{aligned}\frac{\partial L}{\partial \tilde{r}_m^{\mathrm{RF}}} &= 0 \Leftrightarrow \lambda_1\exp\left(\tilde{r}_m^{\mathrm{RF}}\right)+\lambda_{5+N+m}\\ &\quad\times\frac{\exp\left(\tilde{r}_m^{\mathrm{RF}}-\tilde{w}_m\right)\log(2)2^{\exp\left(\tilde{r}_m^{\mathrm{RF}}-\tilde{w}_m\right)/T}}{T\left(2^{\exp\left(\tilde{r}_m^{\mathrm{RF}}-\tilde{w}_m\right)/T}-1\right)}=1-\alpha, \end{aligned} \tag{28}$$

$$\begin{aligned}\frac{\partial L}{\partial \tilde{w}_m} &= 0 \Leftrightarrow -\lambda_5 e^{\tilde{w}_m}-\lambda_{5+N+m}\\ &\quad\times\left(\frac{1}{1+\exp(\tilde{p}_m-\tilde{w}_m)L_m\sigma_\zeta^2 N_0^{-1}}\right.\\ &\quad\left.-\frac{\log(2)\exp\left(\tilde{r}_m-\tilde{w}_m\right)2^{\exp\left(\tilde{r}_m-\tilde{w}_m\right)/T-1}}{T}\right)=0. \end{aligned} \tag{29}$$

2) Layer 2: In each iteration, the LMs are updated by the following expressions:

$$\begin{aligned}\lambda_1^{(i+1)} &= \left[\lambda_1^{(i)}+\hat{\lambda}_1^{(i)}\times\left(\sum_{n=1}^{N}\exp\left(\tilde{r}_n^{\mathrm{VLC}}\right)\right.\right.\\ &\quad\left.\left.+\sum_{m=1}^{M}\exp\left(\tilde{r}_m^{\mathrm{RF}}\right)-C_0\right)\right]^+, \end{aligned} \tag{30}$$

$$\lambda_2^{(i+1)} = \left[\lambda_2^{(i)}+\hat{\lambda}_2^{(i)}\left(\sum_{n=1}^{N}e^{\tilde{P}_n+\tilde{t}_n}-tP_{\mathrm{av}}\right)\right]^+, \tag{31}$$

$$\lambda_3^{(i+1)} = \left[\lambda_3^{(i)}+\hat{\lambda}_3^{(i)}\left(\sum_{m=1}^{M}e^{\tilde{p}_m}-p_{\max}\right)\right]^+, \tag{32}$$

$$\lambda_4^{(i+1)} = \left[\lambda_4^{(i)}+\hat{\lambda}_4^{(i)}\left(\sum_{n=1}^{N}e^{\tilde{t}_n}-t\right)\right]^+, \tag{33}$$

$$\lambda_5^{(i+1)} = \left[\lambda_5^{(i)}+\hat{\lambda}_5^{(i)}\left(\sum_{m=1}^{M}e^{\tilde{w}_m}-w\right)\right]^+, \tag{34}$$

$$\begin{aligned}\lambda_{5+n}^{(i+1)} &= \left[\lambda_{5+n}^{(i)}+\hat{\lambda}_{5+n}^{(i)}\left(\log\left(2^{\exp\left(\tilde{r}_n^{\mathrm{VLC}}-\tilde{t}_n\right)/B}-1\right)\right.\right.\\ &\quad+\log\left(\sigma_\epsilon^2\eta^2+\sigma^2\exp\left(-2\tilde{P}_n\right)\right)\\ &\quad\left.\left.-\log\left(\frac{eh_n^2\eta^2}{2\pi}\right)\right)\right]^+,\\ &\quad\forall n\in\mathcal{N}, \end{aligned} \tag{35}$$

$$\begin{aligned}L &= \alpha\sum_{n=1}^{N}\tilde{r}_n^{\mathrm{VLC}}+(1-\alpha)\sum_{m=1}^{M}\tilde{r}_m^{\mathrm{RF}}-\lambda_1\left(\sum_{n=1}^{N}\exp\left(\tilde{r}_n^{\mathrm{VLC}}\right)+\sum_{m=1}^{M}\exp\left(\tilde{r}_m^{\mathrm{RF}}\right)-C_0\right)\\ &\quad-\lambda_2\left(\sum_{n=1}^{N}e^{\tilde{P}_n+\tilde{t}_n}-tP_{\mathrm{av}}\right)-\lambda_3\left(\sum_{m=1}^{M}e^{\tilde{p}_m}-p_{\max}\right)-\lambda_4\left(\sum_{n=1}^{N}e^{\tilde{t}_n}-t\right)-\lambda_5\left(\sum_{m=1}^{M}e^{\tilde{w}_m}-w\right)\\ &\quad-\sum_{n=1}^{N}\lambda_{5+n}\left(\log\left(2^{\exp\left(\tilde{r}_n^{\mathrm{VLC}}-\tilde{t}_n\right)/B}-1\right)+\log\left(\sigma_\epsilon^2\eta^2+\sigma^2\exp\left(-2\tilde{P}_n\right)\right)-\log\left(\frac{eh_n^2\eta^2}{2\pi}\right)\right)\\ &\quad-\sum_{m=1}^{M}\lambda_{5+N+m}\left(\log\left(2^{\exp\left(\tilde{r}_m^{\mathrm{RF}}-\tilde{w}_m\right)/T}-1\right)+\log\left(\sigma_\zeta^2 L_m+N_0\exp(\tilde{w}_m-\tilde{p}_m)\right)-\log\left(|h_m|^2L_m\right)\right) \end{aligned} \tag{23}$$

$$\lambda_{5+N+m}^{(i+1)} = \Big[\lambda_{5+N+m}^{(i)} + \hat{\lambda}_{5+N+m}^{(i)} \times \left(\log\left(2^{\exp\left(\tilde{r}_m^{\mathrm{RF}} - \tilde{w}_m\right)/T} - 1\right) + \log\left(\sigma_\zeta^2 L_m + N_0 \exp(\tilde{w}_m - \tilde{p}_m)\right) - \log\left(|h_m|^2 L_m\right)\right)\Big]^+, \quad \forall m \in \mathcal{M}, \quad (36)$$

where $[x]^+$ accounts for max(x, 0), $\hat{\lambda}_j^{(i)}$, $j = 1, 2, \ldots, 5 + N + M$ are positive step sizes at iteration i, chosen to satisfy the *diminishing step size rules* [45].

3) The Special Case of Perfect CSI: For the special case of perfect CSI estimation, variances σ_ϵ^2 and σ_ζ^2 are set to 0. Therefore, equations (23), (35) and (36) are simplified and (24) and (25) are reduced to

$$\frac{\partial L}{\partial \tilde{P}_n} = 0 \Leftrightarrow \tilde{P}_n = -\tilde{t}_n \log\left(\frac{\lambda_{5+n}}{\lambda_2}\right), \quad (37)$$

and

$$\frac{\partial L}{\partial \tilde{p}_m} = 0 \Leftrightarrow \tilde{p}_m = \log\left(\frac{\lambda_{5+N+m}}{\lambda_3}\right), \quad (38)$$

respectively. It is noted that the corresponding convex problem can also be solved following a two layer approach, as the one that was presented in Sections III-C1 and III-C2.

Finally, we show the following proposition regarding the equivalence of the original optimization problem in (20) and the transformed convex one in (21).

Proposition 2: The optimization problem in (20) and the optimization problem in (21) are equivalent.

Proof: The two auxiliary variables that are introduced are maximized, as per the transformed objective function. Thus, the data rate variables can be bounded by either the backhaul capacity or the value of the function of rate, constrained by each subsystem resources. To prove rigorously that the two problems are equivalent and the solution of the transformed problem is optimal and not a lower bound, we examine the two aforementioned cases separately.

1) The backhaul capacity C_0 is large enough to accommodate the rates of both subsystems.

This assumption leads C_1 to hold with inequality when optimality is reached. Therefore, due to complementary slackness, $\lambda_1 = 0$. The rest of the Lagrange multipliers cannot be zero, since otherwise the maximization of the dual problem would tend the rates to infinity. Hence, the rest of the constraints hold with equality. More specifically, from C_6 and C_7, we obtain $\exp\left(\tilde{r}_n^{\mathrm{VLC}}\right) = R_n^{\mathrm{VLC}}$ and $\exp\left(\tilde{r}_m^{\mathrm{RF}}\right) = R_m^{\mathrm{RF}}$, $\forall n, m \in \mathcal{N}, \mathcal{M}$, respectively. Note that R_n^{VLC} and R_m^{RF} depend on the resource allocation and they are defined in exactly the same way as in the original problem.

2) The backhaul capacity C_0 bounds the rates of at least one of the subsystems. The first constraint of the problem holds with equality. Since the data rates are bounded by the backhaul capacity, it means that at the resources of at least one of the subsystems are underutilized.

First, we focus on the case that the resources of both subsystems are underutilized. Therefore, C_6 and C_7 will in general hold with inequality, hence the Lagrange multipliers associated with these constraints (λ_{5+n} and λ_{5+N+m}, $\forall n, m \in \mathcal{N}, \mathcal{M}$, respectively) will be zero, due to complementary slackness. By taking into account the KKT conditions (27) and (28) yields

$$\exp\left(\tilde{r}_n^{\mathrm{VLC}}\right) = \frac{\alpha C_0}{N\alpha + M(1-\alpha)} \quad (39)$$

and

$$\exp\left(\tilde{r}_m^{\mathrm{RF}}\right) = \frac{(1-\alpha) C_0}{N\alpha + M(1-\alpha)}, \quad (40)$$

respectively. Similarly, in the original problem, the rates are also bounded by the backhaul capacity, thus, all constraints except C_1 hold with an inequality and their Lagrange multipliers are zero. Then, The Lagrangian of the original problem in this case is:

$$L = \alpha \sum_{n=1}^{N} \log R_n^{\mathrm{VLC}} + (1-\alpha) \sum_{m=1}^{M} \log R_m^{\mathrm{RF}} - \mu_1 \left(\sum_{n=1}^{N} R_n^{\mathrm{VLC}} + \sum_{m=1}^{M} R_m^{\mathrm{RF}} - C_0\right). \quad (41)$$

By taking the KKT conditions, it follows that for the optimal rates it holds:

$$\frac{\partial L}{\partial P_n} = \frac{\alpha}{R_n^{\mathrm{VLC}}} \frac{\partial R_n^{\mathrm{VLC}}}{\partial P_n} - \mu_1 \frac{\partial R_n^{\mathrm{VLC}}}{\partial P_n} = 0 \Rightarrow \frac{\partial R_n^{\mathrm{VLC}}}{\partial P_n} \left(\frac{\alpha}{R_n^{\mathrm{VLC}}} - \mu_1\right) = 0 \Rightarrow R_n^{\mathrm{VLC}} = \frac{\alpha}{\mu_1}, \quad (42)$$

because R_n^{VLC} is an increasing functions of power and its derivative cannot be zero. The same holds for R_m^{RF} with p_m. Since the first constraint of both problems holds with equality, we can calculate λ_1 and μ_1, respectively and we find that they are equal. Therefore, we can get that

$$R_n^{\mathrm{VLC}} = \frac{\alpha C_0}{N\alpha + M(1-\alpha)} = \exp\left(\tilde{r}_n^{\mathrm{VLC}}\right) \quad (43)$$

and

$$R_m^{\mathrm{RF}} = \frac{(1-\alpha) C_0}{N\alpha + M(1-\alpha)} = \exp\left(\tilde{r}_m^{\mathrm{RF}}\right). \quad (44)$$

Furthermore, if one subsystem reaches the limit of its performance due to its resources being depleted and the rate of the other subsystem is limited by the remaining backhaul capacity, it can be shown that the transformed problem is equivalent to the initial one by combining the results from the two aforementioned cases. More specifically, the rates of the subsystem that needs to utilize all the available resources is bounded by either C_6 or C_7, while the remainder of the available backhaul capacity is distributed to the users of the other subsystem. This can easily be proved by taking into account the KKT conditions of the two problems.

Finally, regarding all exponential transformations, it needs to be noticed that the optimal values of the initial variables are higher than zero for each user, otherwise the term of the proportional fairness that corresponds to this user tends to negative infinity. Consequently, the solution set of the initial variables and the equivalent exponential expressions belong in exactly the same set of values, which preserves optimality.

Therefore, we conclude that the two problems are equivalent, so the solution of the transformed problem is also the optimal of the original one. This completes the proof. ■

IV. Simplified Resource Allocation

In this subsection, a simplified version of the proposed optimization problem is presented. In this case, instead of optimizing the timeslot duration and bandwidth that is assigned to each user of the VLC and RF subsystem, respectively, we consider that these resources are equally distributed among the users. Thus, constraint C_2 reduces to

$$\sum_{n=1}^{N} \frac{t_n}{t} P_n \leq P_{\mathrm{av}} \Leftrightarrow \sum_{n=1}^{N} P_n \leq N P_{\mathrm{av}}. \tag{45}$$

Accordingly, the following problem is formulated:

$$\begin{aligned} \max_{\mathbf{P},\mathbf{p}} \ & \alpha \sum_{n=1}^{N} \log\Big(R_n^{[\mathrm{VLC}]}\Big) + (1-\alpha) \sum_{m=1}^{M} \log\Big(R_m^{[\mathrm{RF}]}\Big) \\ \mathbf{s.t.} \ & \mathrm{C}_1 : \sum_{n=1}^{N} R_n^{[\mathrm{VLC}]} + \sum_{m=1}^{M} R_m^{[\mathrm{RF}]} \leq C_0, \\ & \mathrm{C}_2 : \sum_{n=1}^{N} P_n \leq N P_{\mathrm{av}}, \\ & \mathrm{C}_3 : \sum_{m=1}^{M} p_m \leq p_{\max}. \end{aligned} \tag{46}$$

Lemma 1: Problem (46) can be formulated as an equivalent convex optimization problem.

Proof: Problem (46) is essentially a reduced version of problem (20). Following the same steps as in proof of Proposition 1, it readily follows that this problem can be formulated as an equivalent convex optimization problem. ■

The equivalent convex problem is given by

$$\begin{aligned} \max_{\tilde{\mathbf{P}},\tilde{\mathbf{p}},\tilde{\mathbf{r}}^{\mathrm{VLC}},\tilde{\mathbf{r}}^{\mathrm{RF}}} \ & \alpha \sum_{n=1}^{N} \tilde{r}_n^{\mathrm{VLC}} + (1-\alpha) \sum_{m=1}^{M} \tilde{r}_m^{\mathrm{RF}} \\ \mathbf{s.t.} \ & \mathrm{C}_1 : \sum_{n=1}^{N} \exp\left(\tilde{r}_n^{\mathrm{VLC}}\right) + \sum_{m=1}^{M} \exp\left(\tilde{r}_m^{\mathrm{RF}}\right) \leq C_0, \\ & \mathrm{C}_2 : \sum_{n=1}^{N} e^{\tilde{P}_n} \leq N P_{\mathrm{av}}, \\ & \mathrm{C}_3 : \sum_{m=1}^{M} e^{\tilde{p}_m} \leq p_{\max}, \\ & \mathrm{C}_4 : \log\Big(2^{\exp\left(\tilde{r}_n^{\mathrm{VLC}}\right)/(t_n B)} - 1\Big) \\ & \qquad + \log\Big(\sigma_\epsilon^2 \eta^2 + \sigma^2 \exp\Big(-2\tilde{P}_n\Big)\Big) \\ & \qquad \leq \log\Big(\frac{e h_n^2 \eta^2}{2\pi}\Big), \quad \forall n \in \mathcal{N}, \\ & \mathrm{C}_5 : \log\Big(2^{\exp\left(\tilde{r}_m^{\mathrm{RF}}\right)/(w_m T)} - 1\Big) \\ & \qquad + \log\big(\sigma_\zeta^2 L_m + w_m N_0 \exp(-\tilde{p}_m)\big) \\ & \qquad \leq \log\big(|h_m|^2 L_m\big), \quad \forall m \in \mathcal{M}. \end{aligned} \tag{47}$$

TABLE II
Parameters Extracted From [16]

P_{av}	9 W	ρ	1.5
η	0.53 A/W	Ψ_{fov}	$\pi/3$
σ^2	5×10^{-22} A^2	$\Phi_{1/2}$	$\pi/3$
B	40 MHz	p_{max}	1 W
L_r	1 cm^2	W	20 MHz
$T_s(\psi)$	1	N_0	4.002×10^{-21} A^2/W

1) The Special Case of Perfect CSI: Once again, as a special case, the resource allocation problem is studied when perfect CSI estimation is assumed. This ultimately transforms problem (47) to the following:

$$\begin{aligned} \max_{\tilde{\mathbf{P}},\tilde{\mathbf{p}},\tilde{\mathbf{r}}^{\mathrm{VLC}},\tilde{\mathbf{r}}^{\mathrm{RF}}} \ & \alpha \sum_{n=1}^{N} \tilde{r}_n^{\mathrm{VLC}} + (1-\alpha) \sum_{m=1}^{M} \tilde{r}_m^{\mathrm{RF}} \\ \mathbf{s.t.} \ & (47).\mathrm{C}_1, \ (47).\mathrm{C}_2, \ (47).\mathrm{C}_3 \\ & \mathrm{C}_4 : \tilde{P}_n - \frac{1}{2}\log\left(\frac{2^{\exp\left(\tilde{r}_n^{\mathrm{VLC}}\right)/(t_n B)} - 1}{G_n^2}\right) \geq 0, \\ & \qquad \forall n \in \mathcal{N}, \\ & \mathrm{C}_5 : \tilde{p}_m - \log\left(\frac{2^{\exp\left(\tilde{r}_m^{\mathrm{RF}}\right)/(T w_m)} - 1}{A_m^2}\right) \geq 0, \\ & \qquad \forall m \in \mathcal{M}, \end{aligned} \tag{48}$$

which is, in fact, considerably simpler.

V. Simulation Results and Discussion

In this section, Monte Carlo simulation results are presented for a system with a total of 4 users, i.e., 2 VLC users and 2 RF users. This corresponds to a typical scenario for a room, with dimensions 6 m × 6 m × 4 m, with the VLC AP located on the ceiling, in the center of the room, and the RF AP at the center of one of the walls. The locations of the users are random, according to a uniform distribution, in order to fit the aforementioned scenario and the results are averaged out to accommodate the stochastic nature of the problem. Also, the receivers' planes of all VLC users are assumed to be parallels to the transmitter's one. The same parameters as in [16] are considered in the corresponding computer simulations. The correlation coefficients between channel estimation and channel gain in VLC and RF are denoted as ρ_{VLC} and ρ_{RF} respectively. More specifically, the impact of the backhaul capacity C_0, the channel estimation errors, and of α on optimal rates and resource allocation is investigated.

In Fig. 3, the achievable sum rate of the VLC and RF systems are plotted versus the capacity of the backhaul network C_0, when the weight α is equal to 0.5. Practically, this means that neither the VLC system nor the RF one have a priority over the data provided by the backhaul network. In general, it is evident that when the capacity is low enough, RF can reach the same data rate as VLC, and since $\alpha = 0.5$, both subsystems share the capacity equally. However, as C_0 increases, the RF subsystem reaches a ceiling, due to the saturation of the rates that it can achieve with respect to the available transmission power. In addition, we observe that for $C_0 = 2$Gbps, the VLC achievable data rate is 75% better

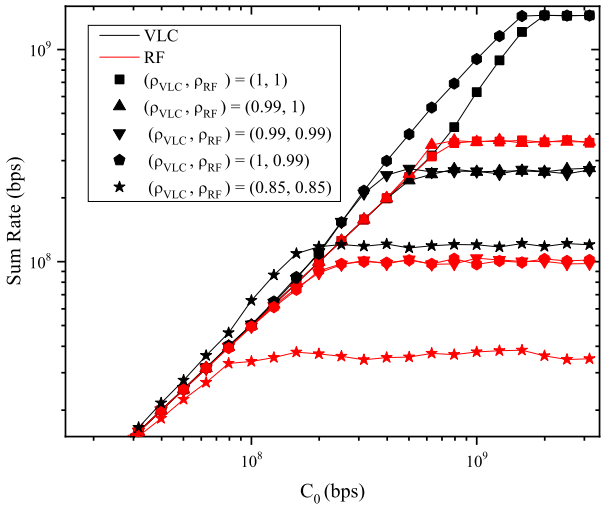

Fig. 3. Sum Rate vs Backhaul Capacity C_0 for $\alpha = 0.5$.

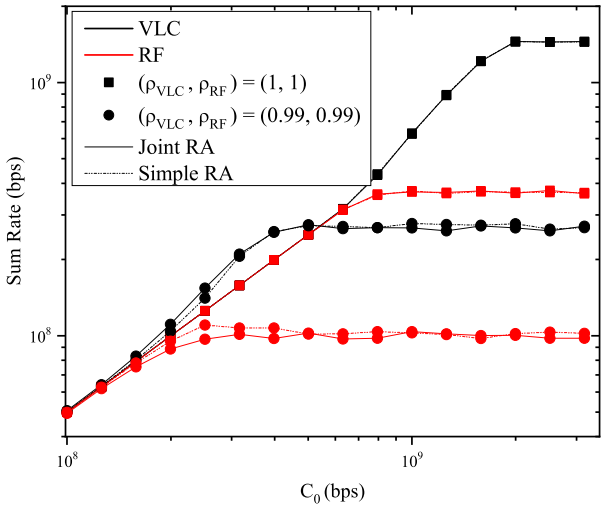

Fig. 4. Comparison between Joint RA and Simple RA in terms of Sum Rate vs Backhaul Capacity C_0 for $\alpha = 0.5$.

than its RF counterpart. Moreover, different channel estimation errors are considered and the pairs can be observed in the figure. As expected, channel estimation errors lead to severe degradation of the achievable sum rate. For example, for $C_0 >$ 2Gbps VLC with perfect CSI achieves at least 80% higher rate than for the case of $\rho_{\mathrm{VLC}} = 0.99$. Aside from this, two interesting remarks need to be derived: First, for the case of perfect CSI at the RF part, imperfect channel estimation at VLC can lead the performance of the VLC subsystem to saturate faster; hence, the achievable sum rate of VLC users turns out to be lower than the RF rate. Secondly, for perfect CSI in VLC, a surpass (up to 68%) is observed when there is imperfect CSI at the RF part. Such a performance is reasonable, since the degradation in the RF subsystem leads to more backhaul capacity available for the VLC system. In this case, the objective function is maximized for a higher value of sum rate at the expense of fairness, since the RF users' data rates are reduced (due to imperfect CSI). However, for higher values of available backhaul capacity, the data rates of the VLC users reach the same ceiling in both cases, due to the saturation of available resources.

In Fig. 4, the comparison between the resource allocation algorithm that jointly optimizes all the available resources of the RF and VLC subsystems, i.e., power, bandwidth and time, marked as Joint RA, and the simplified one, marked as Simple RA, is presented for the case of $\alpha = 0.5$. It can easily be observed that the achievable sum rate of the simple RA follows very closely the one by the joint RA, proving the usefulness of the proposed low-complexity solution, which focuses only on power allocation.

In Fig. 5, a comparison between two cases of imperfect CSI is presented. In one case, resource allocation takes place when the system is aware of the variance of the channel estimation error and in the other case when it is not. It is observed that for lower values of C_0, resource allocation takes into account potential errors in CSI and provides users with more power. In the unknown imperfect CSI case, resource allocation is not handled in the same manner, and the performance of the system is suboptimal. However, for higher backhaul

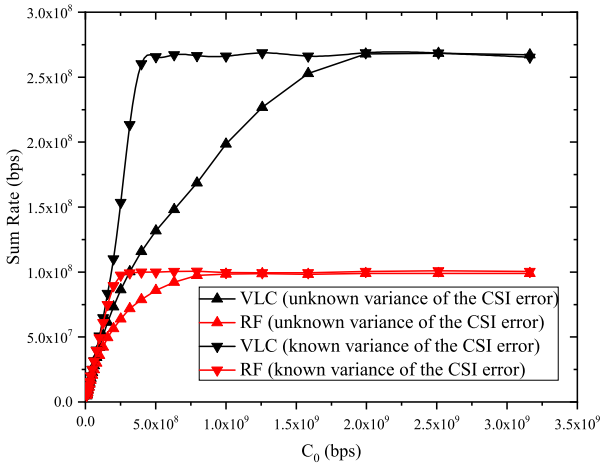

Fig. 5. Sum Rate vs Backhaul Capacity C_0 for $\alpha = 0.5$ assuming imperfect CSI with $\rho_{\mathrm{VLC}} = \rho_{\mathrm{RF}} = 0.99$.

capacity values, both approaches lead to similar resource allocation strategies, hence the comparable sum rate of the two. So, the proposed optimization framework is particularly effective since it gives the opportunity to take into account the imperfect CSI.

Next, we analyze the scenario when the VLC is prioritized over the RF part in the hybrid VLC/RF network. In this case, VLC users will be able to reach higher data rates even when the offered backhaul capacity is low. In Fig. 6, such a comparison between VLC and RF achievable rates is presented for various cases of channel estimation errors. It is shown that VLC subsystem outperforms the RF system for every backhaul capacity value, with VLC achievable data rate being about 75% better than the RF counterpart. However, channel estimation errors degrade severely again the system performance since the RF system with perfect CSI is shown to outperform the VLC system with $\rho_{\mathrm{VLC}} = 0.99$. Some interesting remarks to be made are that perfect CSI for the RF subsystem paired with imperfect CSI for the VLC outperforms the case of perfect CSI for the RF which is paired with perfect CSI for the VLC. This is expected, considering that the performance of

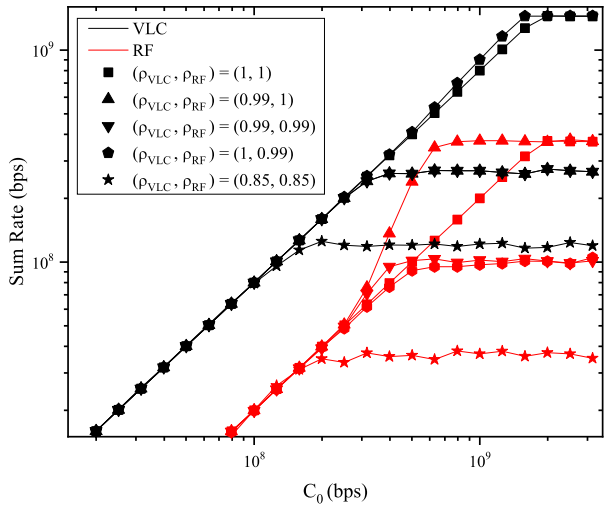

Fig. 6. Sum Rate vs Backhaul Capacity C_0 for $\alpha = 0.8$.

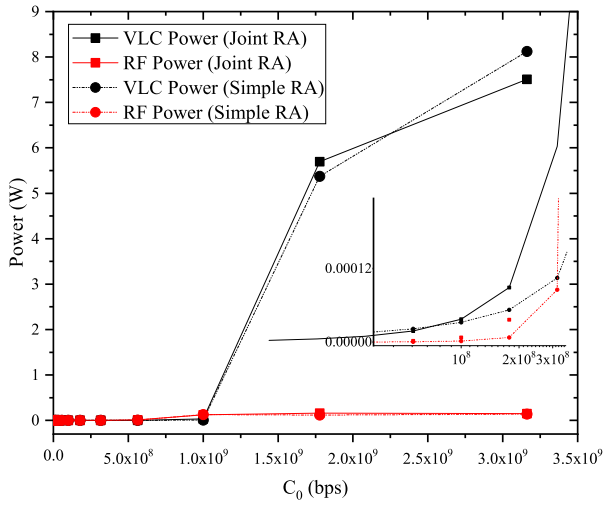

Fig. 7. Average Power vs Backhaul Capacity C_0 for $\alpha = 0.5$.

the VLC subsystem impaired from imperfect channel estimation is degraded, thus making more of the capacity offered from the backhaul network available to be utilized by the RF users. Finally, it can be seen that perfect CSI for VLC paired with a perfect CSI RF exhibits inferior to the case of perfect CSI for the VLC paired with imperfect CSI for the RF only by up to 15%.

Next, we move to the quantification of the power allocation for the hybrid network. In Fig. 7, we examine the power allocation of the $\alpha = 0.5$ case with regards to the capacity of the backhaul network. We observe that, when the VLC and the RF users achieve the same rates, VLC and RF require similar power levels. For higher data rates, which are only achieved by the VLC , as shown in Fig. 3, the power that is consumed by the VLC AP exceeds the power that is consumed by the RF subsystem. Obviously this occurs due to the data rate being much higher for the VLC subsystem. For the case of $\alpha = 0.5$, it appears that the average power that the VLC subsystem consumes is similar to the power needed by the joint resource allocation algorithm. However, when the

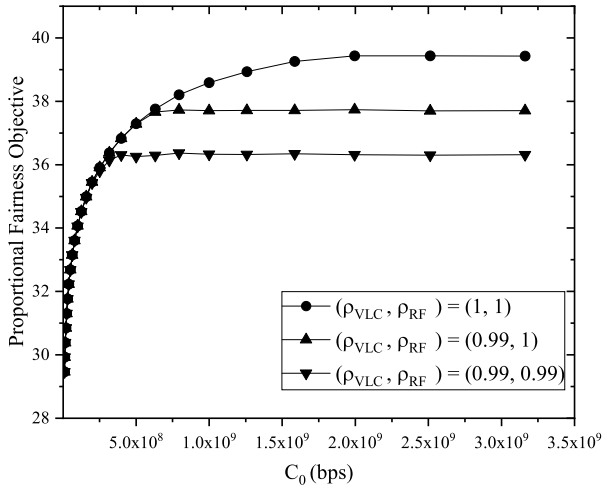

Fig. 8. Proportional Fairness vs Backhaul Capacity C_0 for $\alpha = 0.5$ for different degrees of CSI errors.

VLC system can reach its highest potential, i.e., the backhaul capacity is abundant, the simplified version is more power demanding.

Finally, the maximized proportional fairness (PF) versus the backhaul capacity C_0 is presented in Fig. 8. As it can be observed, similarly to the data rate of the system, as C_0 increases, PF is increased as well, until it reaches a ceiling in each case. We observe that when possible, despite the CSI errors, the performance in terms of PF reaches the same maximum value for both the cases of perfect and imperfect CSI. However, as the CSI errors increase, the impact of which is quantified using the correlation between the actual channel gain and its estimate, the ceiling of the respective PF decreases.

VI. Conclusion

We investigated a hybrid VLC/RF network with the main assumption that both subsystems are served by the same backhaul with limited capacity. Due to the fundamental differences of these two networks, resource allocation in the formed hybrid network is optimized in order to maximize the users' achievable data rate, while also ensuring user fairness. In addition, we considered the case of imperfect CSI in order to quantify the impact of channel estimation errors. Simulation results have illustrated the validity of the proposed analysis and provide useful insights on the impact of the involved parameters on the overall system performance. Finally, a simplified approach to this problem has been proposed, which exhibits comparable results with the complete method but with much less complexity. In future research, a network with multiple access points that operate over the optical and RF bands could be considered, in which case the impact of intra-channel interference to the system performance becomes of paramount importance. More specifically, the two most practical scenarios are a large area with sufficient VLC APs to provide lighting and wireless access coverage, which interfere with each other, or multiple rooms that are divided by walls with an RF AP in each one. In this case, the RF APs interfere with each other, but the VLC APs do not.

APPENDIX
PROOF OF PROPOSITION 1

We commence by transforming the objective function into a concave one. This step is needed since it is a maximization problem. To this end, we introduce two auxiliary variables, r_n^{VLC}, $\forall n \in \mathcal{N}$ and r_m^{RF}, $\forall m \in \mathcal{M}$, respectively, such that

$$r_n^{\mathrm{VLC}} \leq R_n^{[\mathrm{VLC}]} \quad \text{and} \quad r_m^{\mathrm{RF}} \leq R_m^{[\mathrm{RF}]}. \tag{49}$$

The problem of (20) is formulated as

$$\begin{aligned}
\max_{\substack{\mathbf{P},\mathbf{p},\\ \mathbf{r}^{\mathrm{VLC}},\mathbf{r}^{\mathrm{RF}},\mathbf{t},\mathbf{w}}} \quad & \alpha \sum_{n=1}^{N} \log\Big(r_n^{\mathrm{VLC}}\Big) + (1-\alpha) \sum_{m=1}^{M} \log\Big(r_m^{\mathrm{RF}}\Big) \\
\text{s.t.} \quad & \mathrm{C}_1 : \sum_{n=1}^{N} r_n^{\mathrm{VLC}} + \sum_{m=1}^{M} r_m^{\mathrm{RF}} \leq C_0, \\
& \mathrm{C}_2 : \sum_{n=1}^{N} t_n P_n \leq t P_{\mathrm{av}}, \\
& \mathrm{C}_3 : \sum_{m=1}^{M} p_m \leq p_{\max}, \\
& \mathrm{C}_4 : \sum_{n=1}^{N} t_n \leq t, \\
& \mathrm{C}_5 : \sum_{m=1}^{M} w_m \leq w, \\
& \mathrm{C}_6 : r_n^{\mathrm{VLC}} \leq R_n^{[\mathrm{VLC}]}, \forall n \in \mathcal{N}, \\
& \mathrm{C}_7 : r_m^{\mathrm{RF}} \leq R_m^{[\mathrm{RF}]}, \forall m \in \mathcal{M}.
\end{aligned} \tag{50}$$

There are two new constraints, C_6 and C_7 that need to be satisfied due to the use of (49). These new conditions need to be transformed to their convex equivalent as well. In order to continue our proof, we introduce the following transformations:

$$P_n = e^{\tilde{P}_n}, \ \forall n \in \mathcal{N}, \quad \text{and} \quad p_m = e^{\tilde{p}_m}, \ \forall m \in \mathcal{M}. \tag{51}$$

Constraints C_2 and C_3 of (50) are convex because they are both sum of exponentials. Then, the problem of (50) is formulated as

$$\begin{aligned}
\max_{\substack{\tilde{\mathbf{P}},\tilde{\mathbf{p}},\\ \mathbf{r}^{\mathrm{VLC}},\mathbf{r}^{\mathrm{RF}},\mathbf{t},\mathbf{w}}} \quad & \alpha \sum_{n=1}^{N} \log\Big(r_n^{\mathrm{VLC}}\Big) + (1-\alpha) \sum_{m=1}^{M} \log\Big(r_m^{\mathrm{RF}}\Big) \\
\text{s.t.} \quad & \mathrm{C}_1 : \sum_{n=1}^{N} r_n^{\mathrm{VLC}} + \sum_{m=1}^{M} r_m^{\mathrm{RF}} \leq C_0, \\
& \mathrm{C}_2 : \sum_{n=1}^{N} t_n e^{\tilde{P}_n} \leq t P_{\mathrm{av}}, \\
& \mathrm{C}_3 : \sum_{m=1}^{M} e^{\tilde{p}_m} \leq p_{\max}, \\
& \mathrm{C}_4 : \sum_{n=1}^{N} t_n \leq t, \\
& \mathrm{C}_5 : \sum_{m=1}^{M} w_m \leq w, \\
& \mathrm{C}_6 : r_n^{\mathrm{VLC}} \leq R_n^{[\mathrm{VLC}]}, \ \ \forall n \in \mathcal{N}, \\
& \mathrm{C}_7 : r_m^{\mathrm{RF}} \leq R_m^{[\mathrm{RF}]}, \ \ \forall m \in \mathcal{M}.
\end{aligned} \tag{52}$$

However, again, due to the constraints, introduced with the use of (49), i.e., C_6 and C_7, the optimization problem in (50) remains non-convex. Therefore, we also introduce the following transformations

$$\begin{aligned}
r_n^{\mathrm{VLC}} = \exp\Big(\tilde{r}_n^{\mathrm{VLC}}\Big), \ t_n = \exp\big(\tilde{t}_n\big), \\
r_m^{\mathrm{RF}} = \exp\Big(\tilde{r}_m^{\mathrm{RF}}\Big), \text{ and } w_m = \exp\big(\tilde{w}_m\big),
\end{aligned} \tag{53}$$

which transform C_6 as follows:

$$\begin{aligned}
e^{\tilde{r}_n^{\mathrm{VLC}}} \ &\leq \ e^{\tilde{t}_n} B \log_2\left(1 + \frac{e}{2\pi} \frac{h_n^2 \eta^2 \exp\Big(2\tilde{P}_n\Big)}{\sigma_\epsilon^2 \exp\Big(2\tilde{P}_n\Big) + \sigma^2}\right) \\
&\Leftrightarrow 2^{\frac{\exp\left(\tilde{r}_n^{\mathrm{VLC}} - \tilde{t}_n\right)}{B}} - 1 \\
&\leq \ \frac{e h_n^2 \eta^2}{2\pi} \frac{\exp\Big(2\tilde{P}_n\Big)}{\sigma_\epsilon^2 \eta^2 \exp\Big(2\tilde{P}_n\Big) + \sigma^2} \\
&\Leftrightarrow \log\left(2^{\frac{\exp\left(\tilde{r}_n^{\mathrm{VLC}} - \tilde{t}_n\right)}{B}} - 1\right) \\
&\leq \ \log\left(\frac{e h_n^2 \eta^2}{2\pi}\right) + \log\left(\frac{\exp\Big(2\tilde{P}_n\Big)}{\sigma_\epsilon^2 \eta^2 \exp\Big(2\tilde{P}_n\Big) + \sigma^2}\right) \\
&\Leftrightarrow \log\left(2^{\frac{\exp\left(\tilde{r}_n^{\mathrm{VLC}} - \tilde{t}_n\right)}{B}} - 1\right) \\
&\quad + 1 \log\Big(\sigma_\epsilon^2 \eta^2 + \sigma^2 \exp\Big(-2\tilde{P}_n\Big)\Big) \\
&\leq \ \log\left(\frac{e h_n^2 \eta^2}{2\pi}\right).
\end{aligned} \tag{54}$$

The first term of (54), $f = \log(2^{\frac{\exp(\tilde{r}_n^{\mathrm{VLC}} - \tilde{t}_n)}{B}} - 1)$ is convex. This can be obtained by considering its Hessian matrix, which is given by

$$\begin{aligned}
\mathbf{H} &= \begin{bmatrix}
\frac{\partial^2 f}{\partial \tilde{r}_n^{\mathrm{VLC}2}} & \frac{\partial^2 f}{\partial \tilde{r}_n^{\mathrm{VLC}} \partial \tilde{t}_n} & \frac{\partial^2 f}{\partial \tilde{r}_n^{\mathrm{VLC}} \partial \tilde{P}_n} \\
\frac{\partial^2 f}{\partial \tilde{t}_n \partial \tilde{r}_n^{\mathrm{VLC}}} & \frac{\partial^2 f}{\partial \tilde{t}_n^2} & \frac{\partial^2 f}{\partial \tilde{t}_n \partial \tilde{P}_n} \\
\frac{\partial^2 f}{\partial \tilde{P}_n \partial \tilde{r}_n^{\mathrm{VLC}}} & \frac{\partial^2 f}{\partial \tilde{P}_n \tilde{t}_n} & \frac{\partial^2 f}{\partial \tilde{P}_n^2}
\end{bmatrix} \\
&= \begin{bmatrix} q & -q & 0 \\ -q & q & 0 \\ 0 & 0 & 0 \end{bmatrix}.
\end{aligned} \tag{55}$$

It can easily be shown that $\mathbf{H}$ has a non-zero eigenvalue that is expressed by

$$u_1 = q = \frac{2^z z \log(2)(2^z - z\log(2) - 1)}{(2^z - 1)^2}, \tag{56}$$

where z is defined by $z = \frac{\exp\left(\tilde{r}_n^{\mathrm{VLC}} - \tilde{t}_n\right)}{B}$. Considering also that $y = 2^z - z\log(2) - 1$ is an increasing function with respect to z and when $z \to 0$, $y \to 0$, it is shown that

$u_1 \geq 0$. Then, it becomes evident that the Hessian matrix of f is positive semi-definite, due to the fact that the eigenvalues of the matrix are non-negative. Also, the second term, $g = \log(\sigma_\epsilon^2\eta^2 + \sigma^2\exp(-2\tilde{P}_n))$ is convex since its second derivative is positive. After some algebraic manipulations it can be calculated as

$$\frac{d^2 g}{d\tilde{P}_n^2} = \frac{4\eta^2 \exp\left(2\tilde{P}_n\right)\sigma^2\sigma_\epsilon^2}{\left(\eta^2 \exp\left(2\tilde{P}_n\right)\sigma_\epsilon^2 + \sigma^2\right)^2}, \tag{57}$$

and as a result, constraint C_6 is proven to be convex.

Furthermore, the convexity of C_7 is examined; hence, the transformations (53) are applied here yielding

$$\begin{aligned}
\exp\left(\tilde{r}_m^{\mathrm{RF}}\right) &\leq \exp(\tilde{w}_m)\, T \\
&\quad \times \log_2\left(1 + \frac{|h_m|^2 L_m \exp(\tilde{p}_m)}{\exp(\tilde{w}_m)N_0 + \sigma_\zeta^2 L_m \exp(\tilde{p}_m)}\right) \\
&\Leftrightarrow 2^{\frac{\exp\left(\tilde{r}_m^{\mathrm{RF}} - \tilde{w}_m\right)}{T}} - 1 \\
&\leq |h_m|^2 L_m \frac{\exp(\tilde{p}_m)}{\exp(\tilde{w}_m)N_0 + \sigma_\zeta^2 \exp(\tilde{p}_m)} \\
&\Leftrightarrow \log\left(2^{\frac{\exp\left(\tilde{r}_m^{\mathrm{RF}} - \tilde{w}_m\right)}{T}} - 1\right) \\
&\quad + \log\left(\sigma_\zeta^2 L_m + N_0 \exp(\tilde{w}_m - \tilde{p}_m)\right) \\
&\leq \log\left(|h_m|^2 L_m\right),
\end{aligned} \tag{58}$$

which has a very similar form to that one of (54). Following the same steps, we readily prove that constraint C_7 is also convex, which completes the proof.

REFERENCES

[1] V. K. Papanikolaou, P. P. Bamidis, P. D. Diamantoulakis, and G. K. Karagiannidis, "Li-Fi and Wi-Fi with common backhaul: Coordination and resource allocation," in *Proc. IEEE Wireless Commun. Netw. Conf. (WCNC)*, Apr. 2018, pp. 1–6.

[2] M. Kavehrad, "Sustainable energy-efficient wireless applications using light," *IEEE Commun. Mag.*, vol. 48, no. 12, pp. 66–73, Dec. 2010.

[3] S. Arnon, *Visible Light Communication*. Cambridge, U.K.: Cambridge Univ. Press, 2015.

[4] M. Ayyash *et al.*, "Coexistence of WiFi and LiFi toward 5G: Concepts, opportunities, and challenges," *IEEE Commun. Mag.*, vol. 54, no. 2, pp. 64–71, Feb. 2016.

[5] M. Uysal, C. Capsoni, Z. Ghassemlooy, A. Boucouvalas, and E. Udvary, *Optical Wireless Communications: An Emerging Technology*. Cham, Switzerland: Springer, 2016.

[6] *Cisco Visual Networking Index: Forecast and Methodology 2016–2021.(2017)*, Cisco, San Jose, CA, USA, 2017.

[7] I. Stefan and H. Haas, "Hybrid visible light and radio frequency communication systems," in *Proc. IEEE 80th Veh. Technol. Conf. (VTC-Fall)*, Sep. 2014, pp. 1–5.

[8] S. Shao *et al.*, "Design and analysis of a visible-light-communication enhanced WiFi system," *IEEE J. Opt. Commun. Netw.*, vol. 7, no. 10, pp. 960–973, Oct. 2015.

[9] F. Wang, Z. Wang, C. Qian, L. Dai, and Z. Yang, "Efficient vertical handover scheme for heterogeneous VLC-RF systems," *J. Opt. Commun. Netw.*, vol. 7, no. 12, pp. 1172–1180, Dec. 2015.

[10] Y. Wang and H. Haas, "Dynamic load balancing with handover in hybrid Li-Fi and Wi-Fi networks," *J. Lightw. Technol.*, vol. 33, no. 22, pp. 4671–4682, Nov. 15, 2015.

[11] X. Li, R. Zhang, and L. Hanzo, "Cooperative load balancing in hybrid visible light communications and WiFi," *IEEE Trans. Commun.*, vol. 63, no. 4, pp. 1319–1329, Apr. 2015.

[12] X. Wu, M. Safari, and H. Haas, "Access point selection for hybrid Li-Fi and Wi-Fi networks," *IEEE Trans. Commun.*, vol. 65, no. 12, pp. 5375–5385, Dec. 2017.

[13] Y. Wang, X. Wu, and H. Haas, "Load balancing game with shadowing effect for indoor hybrid LiFi/RF networks," *IEEE Trans. Wireless Commun.*, vol. 16, no. 4, pp. 2366–2378, Apr. 2017.

[14] Y. Wang, D. A. Basnayaka, X. Wu, and H. Haas, "Optimization of load balancing in hybrid LiFi/RF networks," *IEEE Trans. Commun.*, vol. 65, no. 4, pp. 1708–1720, Apr. 2017.

[15] G. Pan, J. Ye, and Z. Ding, "Secrecy outage analysis of hybrid VLC-RF systems with light energy harvesting," in *Proc. IEEE 18th Int. Workshop Signal Process. Adv. Wireless Commun. (SPAWC)*, Jul. 2017, pp. 1–5.

[16] D. A. Basnayaka and H. Haas, "Design and analysis of a hybrid radio frequency and visible light communication system," *IEEE Trans. Commun.*, vol. 65, no. 10, pp. 4334–4347, Oct. 2017.

[17] M. R. Zenaidi, Z. Rezki, M. Abdallah, K. A. Qaraqe, and M. S. Alouini, "Achievable rate-region of VLC/RF communications with an energy harvesting relay," in *Proc. IEEE Glob. Commun. Conf. (GLOBECOM)*, Dec. 2017, pp. 1–7.

[18] W. Zhang, L. Chen, X. Chen, Z. Yu, Z. Li, and W. Wang, "Design and realization of indoor VLC-Wi-Fi hybrid network," *J. Commun. Inf. Netw.*, vol. 2, no. 4, pp. 75–87, 2017.

[19] J. Wang, C. Jiang, H. Zhang, X. Zhang, V. C. M. Leung, and L. Hanzo, "Learning-aided network association for hybrid indoor LiFi-WiFi systems," *IEEE Trans. Veh. Technol.*, vol. 67, no. 4, pp. 3561–3574, Apr. 2018.

[20] H. Zhang, N. Liu, K. Long, J. Cheng, V. C. M. Leung, and L. Hanzo, "Energy efficient subchannel and power allocation for the software defined heterogeneous VLC and RF networks," *IEEE J. Sel. Areas Commun.*, vol. 36, no. 3, pp. 658–670, Mar. 2018.

[21] M. Hammouda, S. Akın, A. M. Vegni, H. Haas, and J. Peissig, "Link selection in hybrid RF/VLC systems under statistical queueing constraints," *IEEE Trans. Wireless Commun.*, vol. 17, no. 4, pp. 2738–2754, Apr. 2018.

[22] H. Tabassum and E. Hossain, "Coverage and rate analysis for co-existing RF/VLC downlink cellular networks," *IEEE Trans. Wireless Commun.*, vol. 17, no. 4, pp. 2588–2601, Apr. 2018.

[23] H. Ma, L. Lampe, and S. Hranilovic, "Coordinated broadcasting for multiuser indoor visible light communication systems," *IEEE Trans. Commun.*, vol. 63, no. 9, pp. 3313–3324, Sep. 2015.

[24] H. Marshoud, V. M. Kapinas, G. K. Karagiannidis, and S. Muhaidat, "Non-orthogonal multiple access for visible light communications," *IEEE Photon. Technol. Lett.*, vol. 28, no. 1, pp. 51–54, Jan. 2016.

[25] H. Marshoud, P. C. Sofotasios, S. Muhaidat, G. K. Karagiannidis, and B. S. Sharif, "On the performance of visible light communication systems with non-orthogonal multiple access," *IEEE Trans. Commun.*, vol. 16, no. 10, pp. 6350–6364, Oct. 2017.

[26] A. M. Abdelhady, O. Amin, A. Chaaban, and M.-S. Alouini, "Downlink resource allocation for multichannel TDMA visible light communications," in *Proc. IEEE Glob. Conf. Signal Inf. Process. (GlobalSIP)*, Dec. 2016, pp. 1–5.

[27] G. Pan, P. D. Diamantoulakis, Z. Ma, Z. Ding, and G. K. Karagiannidis, "Simultaneous lightwave information and power transfer: Policies, techniques, and future directions," *IEEE Access*, vol. 7, pp. 28250–28257, 2019.

[28] P. D. Diamantoulakis, G. K. Karagiannidis, and Z. Ding, "Simultaneous lightwave information and power transfer (SLIPT)," *IEEE Trans. Green Commun. Netw.*, vol. 2, no. 3, pp. 764–773, Sep. 2018.

[29] H.-V. Tran, G. Kaddoum, P. D. Diamantoulakis, C. Abou-Rjeily, and G. K. Karagiannidis, "Ultra-small cell networks with collaborative RF and lightwave power transfer," *IEEE Trans. Commun.*, vol. 67, no. 9, pp. 6243–6255, Sep. 2019.

[30] H. Ma, L. Lampe, and S. Hranilovic, "Hybrid visible light and power line communication for indoor multiuser downlink," *IEEE/OSA J. Opt. Commun. Netw.*, vol. 9, no. 8, pp. 635–647, Aug. 2017.

[31] L. Feng, R. Q. Hu, J. Wang, P. Xu, and Y. Qian, "Applying VLC in 5G networks: Architectures and key technologies," *IEEE Netw.*, vol. 30, no. 6, pp. 77–83, Nov./Dec. 2016.

[32] M. Alzenad, M. Z. Shakir, H. Yanikomeroglu, and M. Alouini, "FSO-based vertical backhaul/fronthaul framework for 5G+ wireless networks," *IEEE Commun. Mag.*, vol. 56, no. 1, pp. 218–224, Jan. 2018.

[33] H. Kazemi, M. Safari, and H. Haas, "A wireless optical backhaul solution for optical attocell networks," *IEEE Trans. Wireless Commun.*, vol. 18, no. 2, pp. 807–823, Feb. 2019.

[34] M. Kashef, A. Torky, M. M. Abdallah, N. Al-Dhahir, and K. A. Qaraqe, "On the achievable rate of a hybrid PLC/VLC/RF communication system," in *Proc. IEEE Glob. Commun. Conf. (GLOBECOM)*, Dec. 2015, pp. 1–6.

[35] M. Kashef, M. M. Abdallah, N. Al-Dhahir, and K. A. Qaraqe, "On the impact of PLC backhauling in multi-user hybrid VLC/RF communication systems," in *Proc. IEEE Glob. Commun. Conf. (GLOBECOM)*, 2016, pp. 1–6.
[36] D. Bykhovsky and S. Arnon, "Multiple access resource allocation in visible light communication systems," *J. Lightw. Technol.*, vol. 32, no. 8, pp. 1594–1600, Apr. 15, 2014.
[37] M. S. A. Mossaad, S. Hranilovic, and L. Lampe, "Visible light communications using OFDM and multiple LEDs," *IEEE Trans. Commun.*, vol. 63, no. 11, pp. 4304–4313, Nov. 2015.
[38] T. Komine and M. Nakagawa, "Fundamental analysis for visible-light communication system using LED lights," *IEEE Trans. Consum. Electron.*, vol. 50, no. 1, pp. 100–107, Feb. 2004.
[39] J. M. Kahn and J. R. Barry, "Wireless infrared communications," *Proc. IEEE*, vol. 85, no. 2, pp. 265–298, Feb. 1997.
[40] D. Gu and C. Leung, "Performance analysis of transmit diversity scheme with imperfect channel estimation," *IET Electron. Lett.*, vol. 39, no. 4, pp. 402–403, Feb. 2003.
[41] J.-B. Wang, Q.-S. Hu, J. Wang, M. Chen, and J.-Y. Wang, "Tight bounds on channel capacity for dimmable visible light communications," *J. Lightw. Technol.*, vol. 31, no. 23, pp. 3771–3779, Dec. 1, 2013.
[42] P. D. Diamantoulakis, K. N. Pappi, G. K. Karagiannidis, and H. V. Poor, "Autonomous energy harvesting base stations with minimum storage requirements," *IEEE Wireless Commun. Lett.*, vol. 4, no. 3, pp. 265–268, Jun. 2015.
[43] S. Boyd and L. Vandenberghe, *Convex Optimization*. Cambridge, U.K.: Cambridge Univ. Press, 2004.
[44] L. Vandenberghe, "Subgradients," UCLA, Los Angeles, CA, USA, Lecture Notes of ECE236C, 2019.
[45] S. Boyd, "Subgradient methods," Stanford Univ., Stanford, CA, USA, Lecture notes of EE364b, 2003.

Vasilis K. Papanikolaou (Student Member, IEEE) was born in Kavala, Greece, in 1995. He received the Diploma degree in electrical and computer engineering from the Aristotle University of Thessaloniki, Greece, in 2018, for five years, where is currently pursuing the Ph.D. degree with the Department of Electrical and Computer Engineering. He was a Visitor Researcher with Lancaster University, U.K., and Khalifa University, Abu Dhabi, UAE. His research interests include visible light communications, nonorthogonal multiple access, optimization theory, and game theory. In 2018, he received the IEEE Student Travel Grant Award for IEEE WCNC 2018. He has served as a reviewer in various IEEE journals and conferences.

Panagiotis D. Diamantoulakis (Senior Member, IEEE) received the Diploma (five years) and Ph.D. degrees from the Department of Electrical and Computer Engineering, Aristotle University of Thessaloniki (AUTH), Greece, in 2012 and 2017, respectively. From 2017 to 2019, he was a Visiting Postdoctoral Researcher with the Key Laboratory of Information Coding and Transmission, Southwest Jiaotong University, China, and the Telecommunications Laboratory, Institute for Digital Communications, Friedrich-Alexander-Universität Erlangen-Nürnberg, Germany. Since 2017, he has been a Postdoctoral Fellow with the Wireless Communications Systems Group, AUTH. His current research interests include resource allocation in optical wireless communications, optimization theory and applications, game theory, nonorthogonal multiple access, and wireless power transfer. He serves as an Editor for IEEE WIRELESS COMMUNICATIONS LETTERS, *Physical Communications* (Elsevier), and the IEEE OPEN JOURNAL OF THE COMMUNICATIONS SOCIETY. He was also an Exemplary Reviewer of IEEE COMMUNICATIONS LETTERS in 2014 and the IEEE TRANSACTIONS ON COMMUNICATIONS in 2017 (top 3% of reviewers).

Paschalis C. Sofotasios (Senior Member, IEEE) was born in Volos, Greece, in 1978. He received the M.Eng. degree from Newcastle University, U.K., in 2004, the M.Sc. degree from the University of Surrey, U.K., in 2006, and the Ph.D. degree from the University of Leeds, U.K., in 2011.

He has held academic positions with the University of Leeds, U.K.; the University of California at Los Angeles, Los Angeles, CA, USA; the Tampere University of Technology, Finland; the Aristotle University of Thessaloniki, Greece; and Khalifa University, UAE, where he currently serves as an Assistant Professor with the Department of Electrical Engineering and Computer Science. His M.Sc. degree was funded by a scholarship from U.K.-EPSRC and his Ph.D. degree was sponsored by U.K.-EPSRC and Pace plc. His research interests are physical layer digital and optical wireless communications as well as in topics relating to special functions and statistics. He received the Best Paper Award at ICUFN 2013. He received the Exemplary Reviewer Award from IEEE COMMUNICATIONS LETTERS in 2012 and the IEEE TRANSACTIONS ON COMMUNICATIONS in 2015 and 2016. He serves as an Editor for the IEEE COMMUNICATIONS LETTERS. He serves as a Regular Reviewer for several international journals and has been a member of the Technical Program Committee of numerous IEEE conferences.

Sami Muhaidat (Senior Member, IEEE) received the Ph.D. degree in electrical and computer engineering from the University of Waterloo, Ontario, Canada, in 2006.

From 2007 to 2008, he was an NSERC Postdoctoral Fellow with the Department of Electrical and Computer Engineering, University of Toronto, Canada. From 2008 to 2012, he was an Assistant Professor with the School of Engineering Science, Simon Fraser University, BC, Canada. He is a Professor with Khalifa University, and a Visiting Professor with the Faculty of Engineering, University of Surrey, U.K. His research focuses on wireless communications, optical communications, IoT with emphasis on battery-less devices, and machine learning. He is currently an Area Editor for the IEEE TRANSACTIONS ON COMMUNICATIONS. He also served as a Senior Editor for IEEE COMMUNICATIONS LETTERS, an Editor for the IEEE TRANSACTIONS ON COMMUNICATIONS, and an Associate Editor for the IEEE TRANSACTIONS ON VEHICULAR TECHNOLOGY. He is also a member of Mohammed Bin Rashid Academy of scientists.

George K. Karagiannidis (Fellow, IEEE) was born in Pithagorion, Greece. He received the University Diploma (for five years) and Ph.D. degrees in electrical and computer engineering from the University of Patras in 1987 and 1999, respectively.

From 2000 to 2004, he was a Senior Researcher with the Institute for Space Applications and Remote Sensing, National Observatory of Athens, Greece. In June 2004, he joined the Faculty of the Aristotle University of Thessaloniki, Greece, where he is currently a Professor with the Electrical and Computer Engineering Department and the Director of Digital Telecommunications Systems and Networks Laboratory. He is also an Honorary Professor with South West Jiaotong University, Chengdu, China. He has authored or coauthored more than 500 technical papers published in scientific journals and presented at international conferences. He has authored the Greek edition of a book on *Telecommunications Systems* and coauthored of the book *Advanced Optical Wireless Communications Systems* (Cambridge Publications, 2012). His research interests are in the broad area of digital communications systems and signal processing, with emphasis on wireless communications, optical wireless communications, wireless power transfer and applications, communications for biomedical engineering, stochastic processes in biology, and wireless security.

Prof. Karagiannidis has been involved as the General Chair, the Technical Program Chair, and a member of Technical Program Committees in several IEEE and non-IEEE conferences. In the past, he was an Editor of the IEEE TRANSACTIONS ON COMMUNICATIONS and the *EURASIP Journal of Wireless Communications and Networks* and several times a Guest Editor of IEEE SELECTED AREAS IN COMMUNICATIONS. From 2012 to 2015, he was the Editor-in-Chief of IEEE COMMUNICATIONS LETTERS. He is currently an Associate Editor-in-Chief of the IEEE OPEN JOURNAL OF THE COMMUNICATIONS SOCIETY. He is one of the highly cited authors across all areas of Electrical Engineering, recognized from Clarivate Analytics as Web-of-Science Highly Cited Researcher in the five consecutive years from 2015 to 2019.